Statistical Geometry of Four Calottes on a Sphere

S. Prestipino Giarritta[1] and P. V. Giaquinta[2]

We calculate the configurational integral and reduced distribution functions for a system of four rigid spherical calottes, a model which allows an exact analysis of excluded-volume effects resulting from the interplay between statistics and geometry.

1. INTRODUCTION

The problem of arranging a number of equal rigid particles on a sphere in the most efficient way dates back to Tammes[1] and is of interest in several fields, such as geometry, chemical physics and biology.[2] A statistical mechanical approach to this problem was initially undertaken by Kratky, who introduced the use of spherical boundary conditions and derived the virial equation of state in this non-Euclidean geometry.[3] He also calculated the area of intersection of three spherical calottes.[4] More recently, the statistical thermodynamics of this model was extensively discussed by Post and Glandt,[5,6] who provided the analytical expression of the configurational integral for the three-particle case. Monte Carlo computer simulations have been carried out in order to clarify the extent to which the curvature of the hosting surface modifies the thermodynamic behavior of the model in the region of high densities as compared with the Euclidean case of hard disks on a plane.[7,8] The related question of the random sequential addition of particles onto a spherical surface has also been investigated.[9]

[1] International School for Advanced Studies (SISSA/ISAS), 34013 Trieste, Italy.
[2] Dipartimento di Fisica, Sezione di Fisica Teorica, Università degli Studi di Messina, C.P. 50, 98166 S. Agata-Messina, Italy. GIAQUINT@imeuniv.unime.it.

In this paper we extend the theoretical analysis performed in ref. 5 to include the case of four calottes, further calculating the pair and triplet distribution functions.

The paper is arranged as follows: In Section 2 we introduce the model together with some basic statistical mechanical relations. In Section 3, we review the two- and three-body cases, while the expressions for the configurational integral and for the radial and triplet distribution functions of four calottes are presented in Section 4. The results are discussed in Section 5. Section 6 is finally devoted to concluding remarks.

2. THE MODEL

We consider a system of N equal rigid spherical calottes with curved diameter σ, free to move on the surface of a sphere with radius R. The particle centers interact through the hard-core potential

$$V(1, 2,..., N) = \sum_{i < j} v(d_{ij}) \tag{2.1}$$

where

$$v(d_{ij}) = \begin{cases} +\infty, & d_{ij} < \sigma \\ 0, & d_{ij} > \sigma \end{cases} \tag{2.2}$$

d_{ij} is the distance which is measured along the geodesic joining particles i and j.

The canonical partition function can be written as $Z = Z_{\text{id}} \cdot Q_N$, where Z_{id} is the two-dimensional ideal gas term and

$$Q_N = \frac{1}{(4\pi)^N} \int d\Omega_1 \, d\Omega_2 \cdots d\Omega_N \, e^{-\beta V(1, 2,..., N)} \tag{2.3}$$

is the configurational integral, $d\Omega \equiv \sin \theta \, d\theta \, d\phi$ is the element of solid angle in spherical coordinates, and β is the inverse temperature.

The peculiar interaction we are considering reduces the calculation of the configurational integral to a purely geometrical problem, i.e., "counting" the number of distinct configurations obtained by dropping N equal non-overlapping calottes onto the spherical surface.

We observe that, for given N, Q_N depends on one single parameter $\alpha \equiv \sigma/R$ which is related to the number density via the relation $\rho\sigma^2 = (N/4\pi) \, \alpha^2$. The virial equation of state is obtained from

$$\frac{\beta P}{\rho} = 1 - \left(\frac{\alpha}{2N} \right) \frac{d \ln Q_N}{d\alpha} \tag{2.4}$$

and can be alternatively expressed as[3]

$$\frac{\beta P}{\rho} = 1 + \frac{\pi \rho \sigma^2}{2} \left(\frac{\sin \alpha}{\alpha} \right) g(\alpha) \tag{2.5}$$

where $g(\alpha)$ is the value at contact of the radial distribution function (RDF):

$$g(\theta) = \left(1 - \frac{1}{N} \right) \frac{1}{(4\pi)^{N-2} Q_N} \int d\Omega_3 \cdots d\Omega_N \, e^{-\beta V(1,2,3,...,N)} \tag{2.6}$$

θ is the angular separation between particles 1 and 2.

3. RESULTS FOR TWO AND THREE CALOTTES

3.1. Configurational Integral

The calculation of the thermodynamic properties is quite straightforward for $N = 2$, leading to $Q_2 = \cos^2(\alpha/2)$ and $\beta P/\rho = 1 + (\alpha/4) \, \text{tg}(\alpha/2)$. In this case α ranges between 0 and π.

An expression for the configurational integral of three particles on a sphere has already been given by Post and Glandt.[5] In order to introduce some notations that we shall need later, we shall retrace here the most relevant steps in the calculation of Q_3. However, we shall follow a more direct route than that provided by the virial expansion, finally achieving a more compact analytical result.

Let us fix the relative angular distance θ between particles 1 and 2. Call $\Omega_3(\theta; \alpha)$ the solid angle which is then available to the center of particle 3. It then follows that

$$Q_3 = \frac{1}{8\pi} \int_\alpha^\pi \Omega_3(\theta; \alpha) \sin \theta \, d\theta \tag{3.1}$$

Now, let us indicate as $4R^2 f(\theta; \alpha)$ the area of the surface "slice" shared by a pair of spherical calottes of radius σ separated by a distance $R\theta$ (where $\alpha \leqslant \theta \leqslant 2\alpha$). A simple calculation yields

$$f(\theta; \alpha) = \arcsin \left\{ \cos \left(\frac{\theta}{2} \right) \sin[\tau(\theta; \alpha)] \right\} - \tau(\theta; \alpha) \cos \alpha \tag{3.2}$$

with

$$\tau(\theta; \alpha) \equiv \arccos \left[\frac{\text{tg}(\theta/2)}{\text{tg} \, \alpha} \right] \tag{3.3}$$

After recalling that the area of a calotte with radius σ is $2\pi R^2(1-\cos\alpha)$, we find for $\alpha < \pi/2$

$$\Omega_3(\theta;\alpha) = \begin{cases} 4\pi\cos\alpha + 4f(\theta;\alpha), & \alpha \leqslant \theta \leqslant 2\alpha \\ 4\pi\cos\alpha, & 2\alpha \leqslant \theta \leqslant \pi \end{cases} \tag{3.4}$$

while, in the range $\pi/2 < \alpha < 2\pi/3$, we obtain:

$$\Omega_3(\theta;\alpha) = \begin{cases} 4\pi\cos\alpha + 4f(\theta;\alpha), & \alpha \leqslant \theta \leqslant 2\pi - 2\alpha \\ 0, & 2\pi - 2\alpha \leqslant \theta \leqslant \pi \end{cases} \tag{3.5}$$

For $\alpha > 2\pi/3$, $\Omega_3(\theta;\alpha) = 0$, as it is no longer possible to locate three non-overlapping calottes on the sphere. Let us also note that in the closest-packed arrangement three calottes are centered at the vertices of the equilateral triangle with maximum area inscribed in the sphere.[1,2]

Given Eqs. (3.4) and (3.5), the expression for the configurational integral becomes

$$Q_3 = \begin{cases} \dfrac{1}{2}\cos\alpha\,(1+\cos\alpha) + \dfrac{1}{2\pi}\displaystyle\int_\alpha^{2\alpha} f(\theta;\alpha)\sin\theta\,d\theta, & 0 \leqslant \alpha \leqslant \dfrac{\pi}{2} \\[4mm] \dfrac{1}{2}\cos\alpha\,(-\cos2\alpha+\cos\alpha) + \dfrac{1}{2\pi}\displaystyle\int_\alpha^{2\pi-2\alpha} f(\theta;\alpha)\sin\theta\,d\theta, & \dfrac{\pi}{2} \leqslant \alpha \leqslant \dfrac{2\pi}{3} \end{cases} \tag{3.6}$$

After carrying out explicitly the nontrivial integrals which appear in Eq. (3.6), one arrives at the following result in closed analytical form[10]

$$Q_3 = \frac{3}{4\pi}\cos\alpha\,(1+\cos\alpha)\left[\pi - \arccos\left(\frac{\cos\alpha}{1+\cos\alpha}\right)\right]$$
$$+ \frac{1}{4\pi}(1-\cos\alpha)(1+2\cos\alpha)^{1/2} \tag{3.7}$$

This expression, while being equivalent to the result found by Post and Glandt,[5] is, however, much more compact.[3] The compressibility factor reads

$$\frac{\beta P}{\rho} = 1 + \frac{\alpha\sin\alpha\,(1+2\cos\alpha)}{8\pi Q_3}\left[\pi - \arccos\left(\frac{\cos\alpha}{1+\cos\alpha}\right)\right] \tag{3.8}$$

---

[3] Equation (3.7) differs from Z_3 as given in Appendix B of ref. 5 by a factor A^2. We also note that Eq. (B2) of the cited paper contains a misprint and should in fact be divided by a factor π.

In the limit of vanishing surface curvature ($\alpha \ll 1$), the pressure can be expanded in powers of ρ as

$$\frac{\beta P}{\rho} = 1 + \frac{\pi}{3}\rho\sigma^2 + \left(\frac{\pi^2}{9} - \frac{\sqrt{3}}{18}\pi\right)(\rho\sigma^2)^2 + \mathcal{O}(\rho^3) \tag{3.9}$$

On the other hand, upon expanding the configurational integral of N calottes and then using Eq. (2.4), one arrives at the virial expansion for the pressure:

$$\frac{\beta P}{\rho} = 1 + \sum_{i=1}^{\infty} B_{i+1}(N)\,\rho^i \tag{3.10}$$

where for the first two coefficients one has

$$B_2(N) = \left(1 - \frac{1}{N}\right)B_2 \tag{3.11}$$

$$B_3(N) = \frac{2}{3N}\left(1 - \frac{1}{N}\right)B_2^2 + \left(1 - \frac{1}{N}\right)\left(1 - \frac{2}{N}\right)B_3 \tag{3.12}$$

In order to calculate the infinite-size values B_2 and B_3 one just needs the configurational integral of two and three calottes, respectively. The resulting values are $B_2 = \pi\sigma^2/2$ and $B_3 = (4/3 - \sqrt{3}/\pi)B_2^2$, which reproduce the corresponding virial coefficients of hard disks on a plane. Upon using Eqs. (3.11) and (3.12) for $N = 3$ in Eq. (3.10), one consistently recovers Eq. (3.9).

Now consider the high-density limit. Define $\delta = 2\pi/3 - \alpha$; since for $0 \leqslant \delta \ll 1$

$$\arccos\left(\frac{\cos\alpha}{1 + \cos\alpha}\right) = \pi - 2\cdot 3^{1/4}\sqrt{\delta} + \mathcal{O}(\delta) \tag{3.13}$$

we find

$$Q_3 = \frac{9}{10\pi}\cdot 3^{1/4}\delta^{2.5} + \mathcal{O}(\delta^3) \tag{3.14}$$

so that, in the close-packing limit, the dominant contribution to βP becomes $(5\pi^2/54)(2\pi/3 - \alpha)^{-1}$.

3.2. Radial Distribution Function

From the definition of the RDF one has

$$g(\theta) = \begin{cases} 0, & 0 \leqslant \theta < \alpha \\ \dfrac{1}{6\pi Q_3}\,\Omega_3(\theta;\alpha), & \alpha \leqslant \theta \leqslant \pi \end{cases} \tag{3.15}$$

For $\alpha < \pi/2$, upon inserting the expression for $\Omega_3(\theta; \alpha)$ as given by Eq. (3.4) we obtain

$$g(\theta) = \begin{cases} 0, & 0 \leqslant \theta < \alpha \\ \dfrac{2}{3Q_3}\left[\cos\alpha + \dfrac{1}{\pi}f(\theta;\alpha)\right], & \alpha \leqslant \theta \leqslant 2\alpha \\ \dfrac{2}{3Q_3}\cos\alpha, & 2\alpha \leqslant \theta \leqslant \pi \end{cases} \qquad (3.16)$$

while, for $\pi/2 < \alpha < 2\pi/3$, using Eq. (3.5), it follows that

$$g(\theta) = \begin{cases} 0, & 0 \leqslant \theta < \alpha \\ \dfrac{2}{3Q_3}\left[\cos\alpha + \dfrac{1}{\pi}f(\theta;\alpha)\right], & \alpha \leqslant \theta \leqslant 2\pi - 2\alpha \\ 0, & 2\pi - 2\alpha \leqslant \theta \leqslant \pi \end{cases} \qquad (3.17)$$

We note that, for $\alpha < \pi/2$, given particles 1 and 2 sitting at the north and south poles, respectively, the passage through them of the third particle —along, say, the equatorial ring—is never inhibited. However, as soon as α surpasses this threshold, particles 1 and 2 will be forced by particle 3 to approach each other on a range of angular distances shorter than π. This effect determines the "long-range" vanishing of the RDF. At the same time, particle 3 will no longer be able to pass through particles 1 and 2.

It is easily verified that in both cases (3.16) and (3.17) the RDF is properly normalized:

$$\rho \int R^2 \sin\theta\, g(\theta)\, d\theta\, d\phi = N - 1 \qquad (3.18)$$

with $N = 3$.

4. CONFIGURATIONAL INTEGRAL OF FOUR CALOTTES

Let particle 1 lie at the north pole of the sphere. We assign angular coordinates $(\theta_0, 0)$ and (θ_1, ϕ_1) to particles 2 and 3, respectively. Furthermore, let $\Omega_3(\theta_0; \alpha)$ be the solid angle available to particle 3 given the positions of particles 1 and 2 on the sphere. Correspondingly, $\Omega_4(\theta_0, \theta_1, \phi_1; \alpha)$ is the solid angle accessible to particle 4 after fixing particles 1, 2, and 3. The configurational integral becomes

$$Q_4 = \frac{1}{32\pi^2}\int_\alpha^\pi \sin\theta_0\, d\theta_0 \int_{\Omega_3} \Omega_4(\theta_0, \theta_1, \phi_1; \alpha) \sin\theta_1\, d\theta_1\, d\phi_1 \qquad (4.1)$$

4.1. Low-Density Regime ($\alpha < \pi/2$)

Let us first examine the case $\alpha < \pi/2$. It is convenient to consider the cases $\theta_0 \leqslant 2\alpha$ and $\theta_0 \geqslant 2\alpha$ separately. As a result, $Q_4 = I_1 + I_2$, where

$$I_1 = \frac{1}{32\pi^2} \int_\alpha^{2\alpha} \sin\theta_0 \, d\theta_0 \int_{\Omega_3} \Omega_4(\theta_0, \theta_1, \phi_1; \alpha) \sin\theta_1 \, d\theta_1 \, d\phi_1 \qquad (4.2)$$

$$I_2 = \frac{1}{32\pi^2} \int_{2\alpha}^\pi \sin\theta_0 \, d\theta_0 \int_{\Omega_3} \Omega_4(\theta_0, \theta_1, \phi_1; \alpha) \sin\theta_1 \, d\theta_1 \, d\phi_1 \qquad (4.3)$$

We start by evaluating I_2. To this aim, it is convenient to associate its own excluded-area region to each calotte: such "augmented" calottes (which will be referred to as 1', 2', and 3') may overlap provided that their centers keep at a distance greater than σ. Let A_2 be the area which particle 3' shares with 1' and 2' (corresponding to one or two convex slices of a calotte). It turns out that

$$\Omega_4(\theta_0, \theta_1, \phi_1; \alpha) = 4\pi - \frac{1}{R^2} \left[3 \cdot 2\pi R^2 (1 - \cos\alpha) - A_2\right] \qquad (4.4)$$

so that

$$I_2 = \frac{1}{4} \cos\alpha \, (1 + \cos 2\alpha)(-1 + 3\cos\alpha) + J_2 \qquad (4.5)$$

where

$$J_2 \equiv \frac{1}{32\pi^2} \int_{2\alpha}^\pi \sin\theta_0 \, d\theta_0 \int_{\Omega_3} \frac{A_2}{R^2} \sin\theta_1 \, d\theta_1 \, d\phi_1 \qquad (4.6)$$

The integration domain of the innermost integral in Eq. (4.6) is critically sensitive to both θ_0 and α. According to the value of α, one should first divide the integration interval for θ_0 in subintervals which correspond to different excluded-area geometries as sketched in Fig. 1. The θ_0 partitions considered for the calculation of I_2 are:

(i) $\alpha < \pi/4$: $2\alpha < 3\alpha < 4\alpha < \pi < 2\pi - 4\alpha$.

(ii) $\pi/4 < \alpha < 2\pi/7$: $2\alpha < 3\alpha < 2\pi - 4\alpha < \pi < 4\alpha < 2\pi - 3\alpha$.

(iii) $2\pi/7 < \alpha < \pi/3$: $2\alpha < 2\pi - 4\alpha < 3\alpha < \pi < 2\pi - 3\alpha$.

(iv) $\pi/3 < \alpha < 2\pi/5$: $2\pi - 4\alpha < 2\alpha < 2\pi - 3\alpha < \pi < 3\alpha$.

(v) $2\pi/5 < \alpha < \pi/2$: $2\pi - 3\alpha < 2\alpha < \pi < 3\alpha$.

Here the entries beyond the upper integration limit π have been added in order to help the reader to select the relevant cases. We find
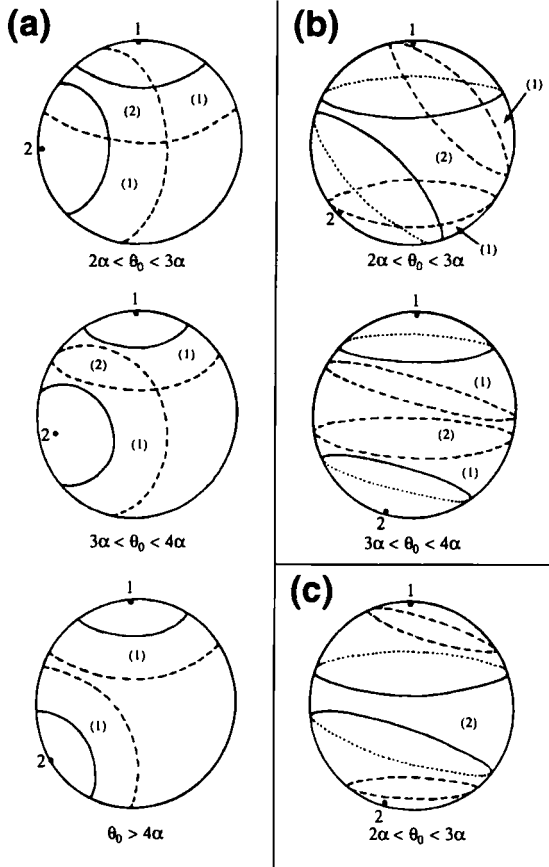
Fig. 1. Excluded-area geometries relevant for the calculation of I_2 in Eq. (4.3). The three sections of the figure refer to the cases (a) $\theta_0 < 2\pi - 4\alpha$, (b) $2\pi - 4\alpha < \theta_0 < 2\pi - 3\alpha$, and (c) $\theta_0 > 2\pi - 3\alpha$. Continuous lines are drawn about the centers (heavy dots) of particles 1 and 2 so as to mark the boundaries of the augmented calottes. Dashed lines represent the loci of points lying 2σ far from the center of each calotte. Numbers within parentheses identify the number of slices contributing to A_2, i.e., to the area which particle $3'$ shares with $1'$ and $2'$, in each integration subregion.

$$
J_2 = \begin{cases}
\dfrac{1}{2\pi}\left[(1 + \cos 2\alpha)\, i_0 - \dfrac{1}{\pi} i_1\right], & 0 < \alpha \leqslant \dfrac{\pi}{3} \\[3mm]
\dfrac{1}{2\pi}\left[(-\cos 3\alpha + \cos 2\alpha)\, i_0 + i_3 - \dfrac{1}{\pi}(i_2 + i_4)\right], & \dfrac{\pi}{3} \leqslant \alpha \leqslant \dfrac{2\pi}{5} \\[3mm]
\dfrac{1}{2\pi}\left(i_5 - \dfrac{1}{\pi} i_6\right), & \dfrac{2\pi}{5} \leqslant \alpha \leqslant \dfrac{\pi}{2}
\end{cases}
\qquad (4.7)
$$

where

$$i_0 \equiv \int_\alpha^{2\alpha} f(\theta; \alpha) \sin \theta \, d\theta = 2\pi [Q_3 - \tfrac{1}{2} \cos \alpha \, (1 + \cos \alpha)] \qquad (4.8a)$$

$$i_1 = \int_{2\alpha}^{3\alpha} \sin \theta_0 \, d\theta_0 \int_{\theta_0 - \alpha}^{2\alpha} f(\theta_1; \alpha) \, \mu(\theta_0, \theta_1; \alpha) \sin \theta_1 \, d\theta_1 \qquad (4.8b)$$

$$i_2 = \int_{2\alpha}^{2\pi - 3\alpha} \sin \theta_0 \, d\theta_0 \int_{\theta_0 - \alpha}^{2\alpha} f(\theta_1; \alpha) \, \mu(\theta_0, \theta_1; \alpha) \sin \theta_1 \, d\theta_1 \qquad (4.8c)$$

$$i_3 = \int_{2\pi - 3\alpha}^{\pi} \sin \theta_0 \, d\theta_0 \int_{\alpha}^{2\pi - \theta_0 - \alpha} f(\theta_1; \alpha) \sin \theta_1 \, d\theta_1 \qquad (4.8d)$$

$$i_4 = \int_{2\pi - 3\alpha}^{\pi} \sin \theta_0 \, d\theta_0 \int_{\theta_0 - \alpha}^{2\pi - \theta_0 - \alpha} f(\theta_1; \alpha) \, \mu(\theta_0, \theta_1; \alpha) \sin \theta_1 \, d\theta_1 \qquad (4.8e)$$

$$i_5 = \int_{2\alpha}^{\pi} \sin \theta_0 \, d\theta_0 \int_{\alpha}^{2\pi - \theta_0 - \alpha} f(\theta_1; \alpha) \sin \theta_1 \, d\theta_1 \qquad (4.8f)$$

$$i_6 = \int_{2\alpha}^{\pi} \sin \theta_0 \, d\theta_0 \int_{\theta_0 - \alpha}^{2\pi - \theta_0 - \alpha} f(\theta_1; \alpha) \, \mu(\theta_0, \theta_1; \alpha) \sin \theta_1 \, d\theta_1 \qquad (4.8g)$$

The function $\mu(\theta_0, \theta_1; \alpha)$, which appears in some of the integrals written above, represents the longitude (in absolute value) of the points lying on the border of calotte 2', having colatitude θ_1:

$$\mu(\theta_0, \theta_1; \alpha) = \arccos \left(\frac{\cos \alpha - \cos \theta_0 \cos \theta_1}{\sin \theta_0 \sin \theta_1} \right) \qquad (4.9)$$

The integrals in Eqs. (4.8b)–(4.8g) are to be evaluated by means of numerical recipes.

We come now to the calculation of I_1. In this case we have

$$\Omega_4(\theta_0, \theta_1, \phi_1; \alpha) = 4\pi - \frac{1}{R^2} [3 \cdot 2\pi R^2 (1 - \cos \alpha) - 4R^2 f(\theta_0; \alpha) - A_1] \qquad (4.10)$$

where the quantity A_1 is to be evaluated according to the overlapping arrangements produced by the augmented calottes 1', 2', and 3'. Such arrangements can take seven different shapes (see Fig. 2). The cases c, d, and e, as well as f and g, are symmetrical.

By inserting the expression (4.10) for $\Omega_4(\theta_0, \theta_1, \phi_1; \alpha)$ into I_1, we get

$$I_1 = \frac{1}{4} \cos \alpha \, (-\cos 2\alpha + \cos \alpha)(-1 + 3 \cos \alpha)$$

$$+ \frac{1}{4\pi} (-1 + 5 \cos \alpha) i_0 + \frac{1}{2\pi^2} i_7 + J_1 \qquad (4.11)$$
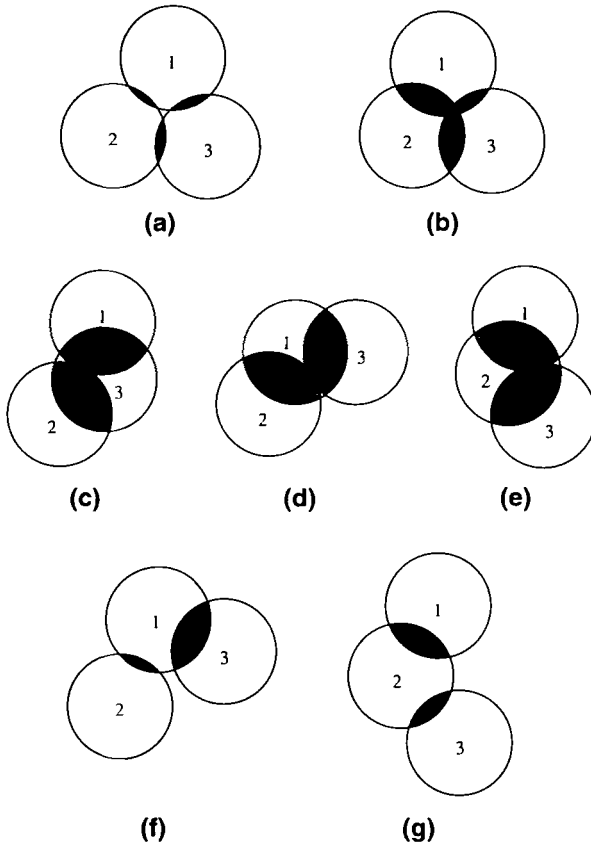
Fig. 2. Sketches of three-particle arrangements with different overlap geometries relevant for the calculation of I_1 in Eq. (4.2). The region $\mathscr{S}$ which is common to pairs of augmented calottes or to all of them has been shaded. Labels used to identify each arrangement are explicitly referred to in the text.

where

$$i_7 = \int_\alpha^{2\alpha} [f(\theta; \alpha)]^2 \sin \theta \, d\theta \tag{4.12}$$

and

$$J_1 = \frac{1}{32\pi^2} \int_\alpha^{2\alpha} \sin \theta_0 \, d\theta_0 \int_{\Omega_3} \frac{A_1}{R^2} \sin \theta_1 \, d\theta_1 \, d\phi_1 \tag{4.13}$$

We are now left with the calculation of J_1. The geometries relevant to the calculation of this quantity are sketched in Fig. 3. In particular, Fig. 3a

refers to the low-density arrangements. The label attached to each shaded zone specifies which case, among those classified in Fig. 2, applies when the center (θ_1, ϕ_1) of calotte 3 falls inside that zone. The continuous line marking the border between the zones a and b is the locus of points lying at distance σ from point $B \equiv \{\theta_0, \tau(\theta_0; \alpha)\}$, while the points belonging to the borderline between the zones c and b are one diameter apart from point $A \equiv \{\theta_0, -\tau(\theta_0; \alpha)\}$. The angles $\theta_0'(\alpha)$ and $\theta_0''(\alpha)$, which are referred to in
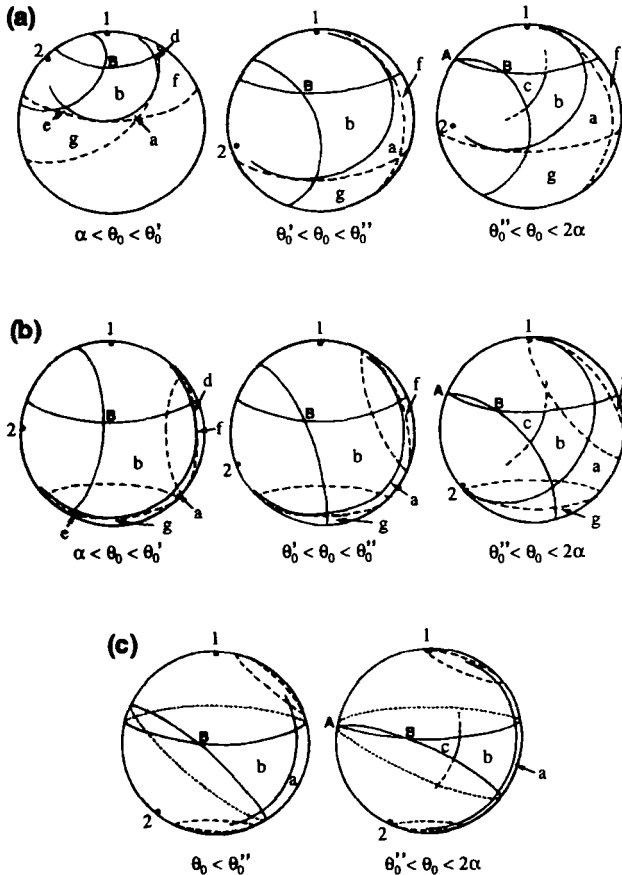
Fig. 3. Excluded-area geometries relevant for the calculation of I_1 in Eq. (4.2). The three sections of the figure refer to the cases (a) $\theta_0 < 2\pi - 4\alpha$, (b) $2\pi - 4\alpha < \theta_0 < 2\pi - 3\alpha$, (c) $\theta_0 > 2\pi - 3\alpha$. The continuous lines centered on particles 1 and 2 mark the boundaries of each augmented calotte. Dashed lines represent the loci of points lying 2σ far from the center of each calotte. See the discussion in the text for further details.

Fig. 3, fulfill the conditions $\mu(\theta_0', 2\alpha; \alpha) = \tau(\theta_0'; \alpha)$ and $\text{dist}(A, B) = \sigma$, respectively. Upon carrying out the calculations, we obtain

$$\theta_0'(\alpha) = \arccos[\cos \alpha \, (2 \cos \alpha - 1)] \qquad (4.14a)$$

$$\theta_0''(\alpha) = \arccos\left(\frac{4 \cos^2 \alpha - \cos \alpha - 1}{\cos \alpha + 1}\right) \qquad (4.14b)$$

A plot of these functions is shown in Fig. 4. We note that $\alpha < \theta_0' < \theta_0'' < 2\alpha$ whenever $0 < \alpha < \pi/2$. Furthermore, the following inequalities hold:

   (i) $\alpha < \pi/3$: $\alpha < 2\alpha < 2\pi - 4\alpha < 2\pi - 3\alpha$.

   (ii) $\pi/3 < \alpha < 2\pi/5$: $\alpha < 2\pi - 4\alpha < 2\alpha < 2\pi - 3\alpha$.

   (iii) $2\pi/5 < \alpha < \pi/2$: $2\pi - 4\alpha < \alpha < \theta_0' < 2\pi - 3\alpha < 2\alpha$.

So far we have identified different integration regions, but we have not yet specified the structure of the integrand. To this end, let s_{12} represent the area of the slice common to calottes 1′ and 2′, i.e., $4R^2 f(\theta_0; \alpha)$, and the same for s_{13} and s_{23}. We now consider each of the cases presented in Fig. 2 separately:

$$a \to A_1 = s_{13} + s_{23}$$

$$b \to A_1 = s_{13} + s_{23} - \zeta$$

$$c \to A_1 = s_{13} + s_{23} - s_{12}$$

$$d, f \to A_1 = s_{13}$$

$$e, g \to A_1 = s_{23}$$
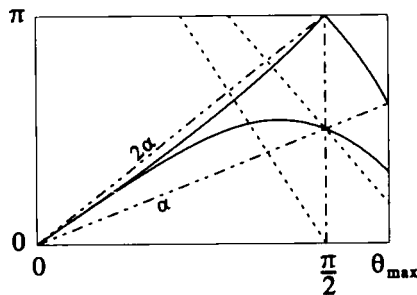
Fig. 4.   The angles θ_0' (lower continuous line) and θ_0'' (upper continuous line), as given by Eqs. (4.14a) and (4.14b), plotted as a function of α up to $\theta_{max} \equiv \arccos(-1/3)$. The angles $2\pi - 4\alpha$ and $2\pi - 3\alpha$ are also shown as dashed lines.

where ζ is the area of the region common to all of the three calottes $1'$, $2'$, and $3'$. Let T be the region of the spherical surface which is covered by calottes $1'$, $2'$, and $3'$. We find

$$\zeta = A(T) - 3 \cdot 2\pi R^2 (1 - \cos \alpha) + s_{12} + s_{13} + s_{23} \qquad (4.15)$$

where $A(T)$ is the area of T. Consider now the decomposition of T as shown in Fig. 5: it is clear that the calculation of $A(T)$ becomes possible as soon as one calculates the internal angles of the triangle whose vertices are the particle centers of calottes 1, 2, and 3. The values of the angles centered at 1, 2, and 3 are ϕ_1, $\xi(\theta_0, \theta_1, \phi_1)$, and $\xi(\theta_1, \theta_0, \phi_1)$, respectively. The calculation of $\xi_{01} \equiv \xi(\theta_0, \theta_1, \phi_1)$ is easier if one resorts to a reference frame transformation whose effect is moving particle 2 onto the north pole of the sphere. The result is

$$\xi_{01} = \arccos \left[\frac{\sin \theta_0 \cos \theta_1 - \sin \theta_1 \cos \theta_0 \cos \phi_1}{[(\sin \theta_0 \cos \theta_1 - \sin \theta_1 \cos \theta_0 \cos \phi_1)^2 + \sin^2 \theta_1 \sin^2 \phi_1]^{1/2}} \right]$$

$$(4.16)$$
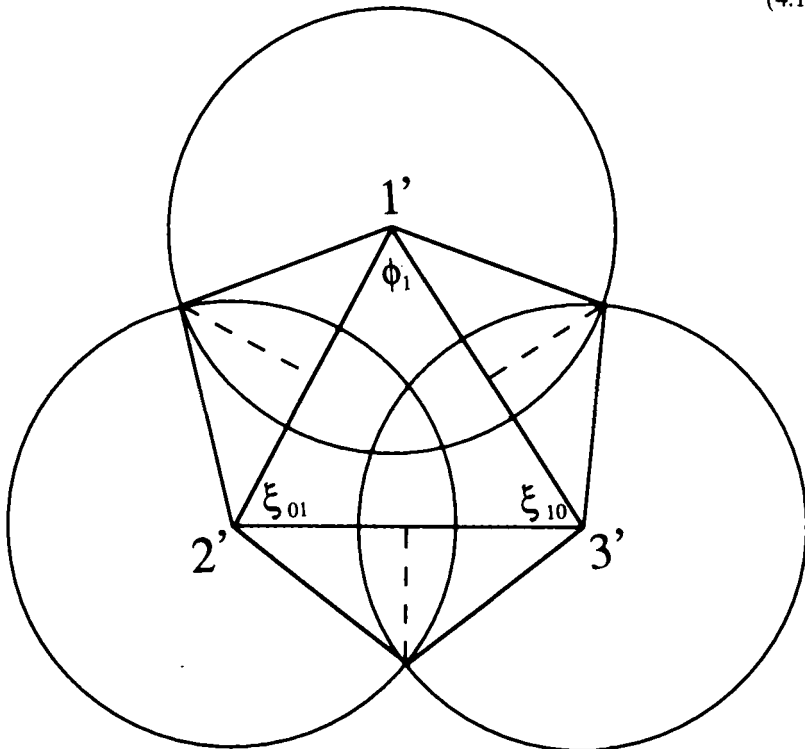
Fig. 5. A geometrical construction useful for the calculation of the area $A(T)$ which appears in Eq. (4.15).

and the expression for ζ finally reads

$$\zeta = \tfrac{1}{2}(s_{12} + s_{13} + s_{23}) - \pi R^2 + R^2(\phi_1 + \xi_{10} + \xi_{01}) \cos \alpha \qquad (4.17)$$

After noting that symmetry considerations imply that

$$\int_{e+g} s_{23} = \int_{d+f} s_{13} \qquad (4.18a)$$

$$\int_{a,b,c} (s_{13} + s_{23}) = 2 \int_{a,b,c} s_{13} \qquad (4.18b)$$

and

$$R^2 \int_b (\phi_1 + \xi_{01}) = 2R^2 \int_b \phi_1 \qquad (4.18c)$$

we can write J_1 in the form $J_1 = (1/2\pi)(K_1 + K_2 + K_3)$, where K_1 refers to the contributions resulting from regions labeled a, d, e, f, and g in Fig. 3, while K_2 and K_3 are associated with regions c and b, respectively. We obtain

$$K_1 = \begin{cases} (-\cos 2\alpha + \cos \alpha) \, i_0 - \dfrac{1}{\pi} i_8, & 0 \leqslant \alpha \leqslant \dfrac{2\pi}{5} \\[2mm] (-\cos 3\alpha + \cos \alpha) \, i_0 + i_{10} - \dfrac{1}{\pi}(i_9 + i_{11}), & \dfrac{2\pi}{5} \leqslant \alpha \leqslant \dfrac{\pi}{2} \end{cases} \qquad (4.19a)$$

$$K_2 = \frac{1}{2\pi} i_{12} \qquad (4.19b)$$

$$K_3 = \frac{1}{4\pi}(i_{13} + i_{15}) - \frac{1}{8\pi}(i_{14} + i_{16}) \cos \alpha \qquad (4.19c)$$

The quantities i_n which enter Eqs. (4.19a)–(4.19c) are defined as

$$i_8 = \int_\alpha^{2\alpha} \sin \theta_0 \, d\theta_0 \int_\alpha^{2\alpha} f(\theta_1; \alpha) \, \beta(\theta_0, \theta_1; \alpha) \sin \theta_1 \, d\theta_1 \qquad (4.20a)$$

$$i_9 = \int_\alpha^{2\pi - 3\alpha} \sin \theta_0 \, d\theta_0 \int_\alpha^{2\alpha} f(\theta_1; \alpha) \, \beta(\theta_0, \theta_1; \alpha) \sin \theta_1 \, d\theta_1 \qquad (4.20b)$$

$$i_{10} = \int_{2\pi - 3\alpha}^{2\alpha} \sin \theta_0 \, d\theta_0 \int_\alpha^{2\pi - \theta_0 - \alpha} f(\theta_1; \alpha) \sin \theta_1 \, d\theta_1 \qquad (4.20c)$$

$$i_{11} = \int_{2\pi - 3\alpha}^{2\alpha} \sin \theta_0 \, d\theta_0 \int_\alpha^{2\pi - \theta_0 - \alpha} f(\theta_1; \alpha) \, \beta(\theta_0, \theta_1; \alpha) \sin \theta_1 \, d\theta_1 \qquad (4.20d)$$

$$= \int_{\theta_0^-}^{2\alpha} \sin \theta_0 \, d\theta_0 \int_{\alpha}^{\psi''} [2f(\theta_1; \alpha) - f(\theta_0; \alpha)]$$

$$\times [-\tau_0 + \tau_1 - \mu(\theta_0, \theta_1; \alpha)] \sin \theta_1 \, d\theta_1 \tag{4.20e}$$

$$i_{13} = \int_{\theta_0^-}^{2\alpha} \sin \theta_0 \, d\theta_0 \int_{\alpha}^{\psi'} \left[2f(\theta_1; \alpha) - f(\theta_0; \alpha) + \frac{\pi}{2} \right]$$

$$\times [\tau_0 + \tau_1 - \gamma(\theta_0, \theta_1; \alpha)] \sin \theta_1 \, d\theta_1 \tag{4.20f}$$

$$i_{14} = \int_{\theta_0^-}^{2\alpha} \sin \theta_0 \, d\theta_0 \int_{\alpha}^{\psi'} \sin \theta_1 \, d\theta_1 \int_{\gamma}^{\tau_0 + \tau_1} (2\phi_1 + \xi_{10}) \, d\phi_1 \tag{4.20g}$$

$$i_{15} = \int_{\alpha}^{\theta_0^-} \sin \theta_0 \, d\theta_0 \int_{\alpha}^{2\alpha} \left[2f(\theta_1; \alpha) - f(\theta_0; \alpha) + \frac{\pi}{2} \right]$$

$$\times [\tau_0 + \tau_1 - \delta(\theta_0, \theta_1; \alpha)] \sin \theta_1 \, d\theta_1 \tag{4.20h}$$

$$i_{16} = \int_{\alpha}^{\theta_0^-} \sin \theta_0 \, d\theta_0 \int_{\alpha}^{2\alpha} \sin \theta_1 \, d\theta_1 \int_{\delta}^{\tau_0 + \tau_1} (2\phi_1 + \xi_{10}) \, d\phi_1 \tag{4.20i}$$

where $\tau_0 \equiv \tau(\theta_0; \alpha)$, $\tau_1 \equiv \tau(\theta_1; \alpha)$, and

$$\beta(\theta_0, \theta_1; \alpha) = \max\{\tau_0 + \tau_1, \mu\} \tag{4.21}$$

$$\gamma \equiv \gamma(\theta_0, \theta_1; \alpha) = \max\{-\tau_0 + \tau_1, \mu\} \tag{4.22}$$

$$\delta \equiv \delta(\theta_0, \theta_1; \alpha) = \max\{\tau_0 - \tau_1, \mu\} \tag{4.23}$$

We have also indicated the value of θ_1 when $\tau_0 + \tau_1 = \mu$ as $\psi' \equiv \psi'(\theta_0; \alpha)$, while $\psi'' \equiv \psi''(\theta_0; \alpha)$ is defined through the condition $-\tau_0 + \tau_1 = \mu$.

It is possible to verify that, in the limit of very low density, to order α^4

$$Q_4 \simeq \frac{1}{4} \cos \alpha \, (1 + \cos \alpha)(-1 + 3 \cos \alpha) + \frac{1}{4\pi} (1 + 7 \cos \alpha) \, i_0$$

$$= 1 - \frac{3}{2} \alpha^2 + \left(\frac{13}{16} + \frac{3\sqrt{3}}{16\pi} \right) \alpha^4 + \cdots \tag{4.24}$$

Correspondingly,

$$\frac{\beta P}{\rho} = 1 + \frac{3\pi}{8} (\rho\sigma^2) + \left(\frac{5}{32} \pi^2 - \frac{3\sqrt{3}}{32} \pi \right) (\rho\sigma^2)^2 + \cdots \tag{4.25}$$

in accordance with the size-dependence rule for the second and third virial coefficients.

4.2. High-Density Regime ($\alpha > \pi/2$)

As will become readily clear, the high-density case is relatively simpler than the low-density one. The solid angle which is in principle available to the centers of particles 3 and 4, after dropping particles 1 and 2 on the sphere, is the cap slice which in Fig. 6 is delimited by the points A, B, C, D. It is obvious that when dist$(A, B) < \sigma$ (i.e., for $\theta_0 > \theta_0''$), it is no longer possible to accommodate four particles on the sphere. We also observe that, if $\alpha > \pi/2$, then $\tau_0 > \pi/2$ and $\tau_0 + \tau_1 > \pi$. Now, let us indicate the angle θ_1 which satisfies the equation $2\pi - \tau_0 - \tau_1 = \mu$ as $\tilde{\psi} \equiv \tilde{\psi}(\theta_0; \alpha)$. Given $\theta_0 < \theta_0''$, the locus of points which lie a distance greater than σ from point A (or B) is defined through the conditions $\alpha < \theta_1 < \tilde{\psi}(\theta_0; \alpha)$ and $\mu < \phi_1 < 2\pi - \tau_0 - \tau_1$ (or $\tau_0 + \tau_1 < \phi_1 < 2\pi - \mu$). It thus follows that, for $\alpha > \pi/2$, the configurational space available to the centers of the two calottes 3 and 4 is no longer connected whatever the relative position of particles 1 and 2 on the sphere. Conversely, for $\alpha < \pi/2$, it is always possible to find some configurations of particles 1 and 2 which allow the dynamical exchange of particles 3 and 4 (as, for instance, in a diametrically opposite setup of 1 and 2). In other words, for $\alpha = \pi/2$, the system undergoes a spontaneous "confinement transition" which ultimately leads to a rigid tetrahedral structure when α attains its maximum value, i.e., arccos$(-1/3) \simeq 109°.47$, a result which precisely follows from the condition $\alpha = \theta_0''(\alpha)$.

(a)   **(b)**
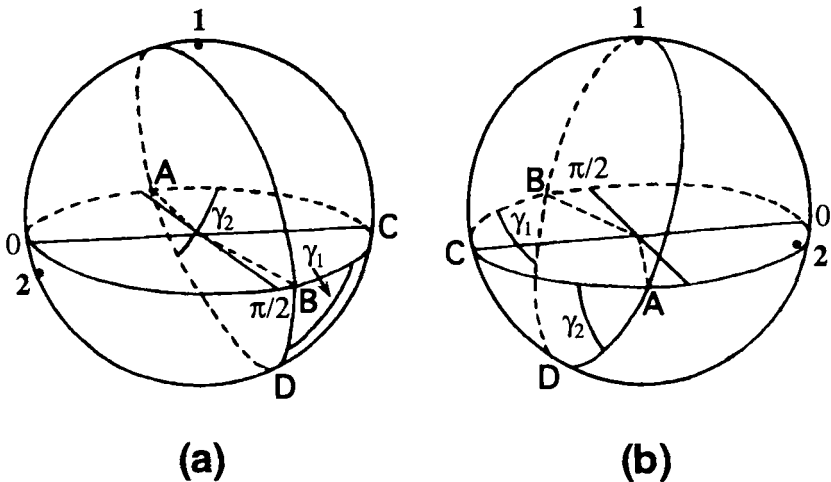
Fig. 6. (a) Front and (b) rear views of the sphere for $\alpha > \pi/2$ with the indication of the solid angle available to the centers of particles 3 and 4. The arcs γ_1 and γ_2 are at distance σ from A and B, respectively.

Adopting the same notations as before, we find

$$Q_4 = \frac{1}{32\pi^2} \int_\alpha^{\theta_0''} \sin\theta_0 \, d\theta_0 \int_\alpha^{\bar\psi} \sin\theta_1 \, d\theta_1 \int_\mu^{2\pi-\tau_0-\tau_1} \left[4\pi - \frac{1}{R^2} A(T) \right] d\phi_1$$

$$+ \frac{1}{32\pi^2} \int_\alpha^{\theta_0''} \sin\theta_0 \, d\theta_0 \int_\alpha^{\bar\psi} \sin\theta_1 \, d\theta_1 \int_{\tau_0+\tau_1}^{2\pi-\mu} \left[4\pi - \frac{1}{R^2} A(T) \right] d\phi_1$$

(4.26)

or

$$Q_4 = \frac{1}{16\pi^2} \left(i_{17} - i_{18} \cos\alpha \right)$$ (4.27)

where

$$i_{17} = \int_\alpha^{\theta_0''} \sin\theta_0 \, d\theta_0 \int_\alpha^{\bar\psi} \left[-\pi + 6\pi \cos\alpha + 2f(\theta_0; \alpha) + 4f(\theta_1; \alpha) \right]$$

$$\times (2\pi - \tau_0 - \tau_1 - \mu) \sin\theta_1 \, d\theta_1$$ (4.28a)

$$i_{18} = \int_\alpha^{\theta_0''} \sin\theta_0 \, d\theta_0 \int_\alpha^{\bar\psi} \sin\theta_1 \, d\theta_1 \int_\mu^{2\pi-\tau_0-\tau_1} (2\phi_1 + \xi_{10}) \, d\phi_1$$ (4.28b)

4.3. Radial Distribution Function

The following expression for the RDF holds:

$$g(\theta_0) = \begin{cases} 0, & 0 \leqslant \theta_0 < \alpha \\ \dfrac{3}{64\pi^2 Q_4} \displaystyle\int_{\Omega_3} \Omega_4(\theta_0, \theta_1, \phi_1; \alpha) \sin\theta_1 \, d\theta_1 \, d\phi_1, & \alpha \leqslant \theta_0 \leqslant \pi \end{cases}$$ (4.29)

In order to calculate the integral in $g(\theta_0)$, we must consider the cases $\alpha < \pi/2$ and $\alpha > \pi/2$ separately, as already done for the calculation of Q_4.

Let us first assume $\alpha < \pi/2$. For $\theta_0 \geqslant 2\alpha$, we need to distinguish three subranges for α:

$$\alpha < \frac{\pi}{3}: \quad g(\theta_0) = \begin{cases} h_2(\alpha) + \dfrac{3}{4\pi Q_4} \left(g_0 - \dfrac{1}{\pi} g_2 \right), & 2\alpha \leqslant \theta_0 \leqslant 3\alpha \\ h_2(\alpha) + \dfrac{3}{4\pi Q_4} g_0, & 3\alpha \leqslant \theta_0 \leqslant \pi \end{cases}$$ (4.30a)

$$\frac{\pi}{3} < \alpha < \frac{2\pi}{5}: \quad g(\theta_0) = \begin{cases} h_2(\alpha) + \dfrac{3}{4\pi Q_4}\left(g_0 - \dfrac{1}{\pi}g_2\right), & 2\alpha \leqslant \theta_0 \leqslant 2\pi - 3\alpha \\[3mm] h_2(\alpha) + \dfrac{3}{4\pi Q_4}\left(g_1 - \dfrac{1}{\pi}g_3\right), & 2\pi - 3\alpha \leqslant \theta_0 \leqslant \pi \end{cases}$$

$$\text{(4.30b)}$$

$$\frac{2\pi}{5} < \alpha < \frac{\pi}{2}: \quad g(\theta_0) = h_2(\alpha) + \frac{3}{4\pi Q_4}\left(g_1 - \frac{1}{\pi}g_3\right) \tag{4.30c}$$

where $h_2(\alpha) \equiv (3/8Q_4)\cos\alpha\,(-1 + 3\cos\alpha)$, and

$$g_0 = \int_\alpha^{2\alpha} f(\theta;\alpha)\sin\theta\,d\theta = i_0 \tag{4.31a}$$

$$g_1 = \int_\alpha^{2\pi - \theta_0 - \alpha} f(\theta;\alpha)\sin\theta\,d\theta \tag{4.31b}$$

$$g_2 = \int_{\theta_0 - \alpha}^{2\alpha} f(\theta_1;\alpha)\,\mu(\theta_0,\theta_1;\alpha)\sin\theta_1\,d\theta_1 \tag{4.31c}$$

$$g_3 = \int_{\theta_0 - \alpha}^{2\pi - \theta_0 - \alpha} f(\theta_1;\alpha)\,\mu(\theta_0,\theta_1;\alpha)\sin\theta_1\,d\theta_1 \tag{4.31d}$$

On the other hand, after defining the auxiliary function

$$h_1(\theta_0;\alpha) \equiv \frac{3}{8Q_4}\cos\alpha\,(-1 + 3\cos\alpha)$$

$$+ \frac{3}{8\pi Q_4}\,(-1 + 5\cos\alpha)\,f(\theta_0;\alpha) + \frac{3}{4\pi^2 Q_4}\,f(\theta_0;\alpha)^2$$

it follows for $\alpha \leqslant \theta_0 \leqslant 2\alpha$:

$\alpha < 2\pi/5$:

$$g(\theta_0) = \begin{cases} 0, & 0 \leqslant \theta_0 < \alpha \\[3mm] h_1(\theta_0;\alpha) + \dfrac{3}{16\pi^2 Q_4}\left(4\pi g_0 - 4g_4 + g_7 - \dfrac{1}{2}g_8\cos\alpha\right), \\[1mm] \qquad \alpha \leqslant \theta_0 \leqslant \theta_0' \\[3mm] h_1(\theta_0;\alpha) + \dfrac{3}{16\pi^2 Q_4}\left(4\pi g_0 - 4g_4 + g_9 - \dfrac{1}{2}g_{10}\cos\alpha\right), \\[1mm] \qquad \theta_0' \leqslant \theta_0 \leqslant \theta_0'' \\[3mm] h_1(\theta_0;\alpha) + \dfrac{3}{16\pi^2 Q_4}\left(4\pi g_0 - 4g_4 + 2g_6 + g_9 - \dfrac{1}{2}g_{10}\cos\alpha\right), \\[1mm] \qquad \theta_0'' \leqslant \theta_0 \leqslant 2\alpha \end{cases} \tag{4.32a}$$

$2\pi/5 < \alpha < \alpha^*$:

$$g(\theta_0) = \begin{cases} 0, & 0 \leqslant \theta_0 < \alpha \\[2mm] h_1(\theta_0;\alpha) + \dfrac{3}{16\pi^2 Q_4}\left(4\pi g_0 - 4g_4 + g_7 - \dfrac{1}{2}g_8 \cos\alpha\right), \\[2mm] \qquad \alpha \leqslant \theta_0 \leqslant \theta_0' \\[2mm] h_1(\theta_0;\alpha) + \dfrac{3}{16\pi^2 Q_4}\left(4\pi g_0 - 4g_4 + g_9 - \dfrac{1}{2}g_{10} \cos\alpha\right), \\[2mm] \qquad \theta_0' \leqslant \theta_0 \leqslant \theta_0'' \\[2mm] h_1(\theta_0;\alpha) + \dfrac{3}{16\pi^2 Q_4}\left(4\pi g_0 - 4g_4 + 2g_6 + g_9 - \dfrac{1}{2}g_{10} \cos\alpha\right), \\[2mm] \qquad \theta_0'' \leqslant \theta_0 \leqslant 2\pi - 3\alpha \\[2mm] h_1(\theta_0;\alpha) + \dfrac{3}{16\pi^2 Q_4}\left(4\pi g_1 - 4g_5 + 2g_6 + g_9 - \dfrac{1}{2}g_{10} \cos\alpha\right), \\[2mm] \qquad 2\pi - 3\alpha \leqslant \theta_0 \leqslant 2\alpha \end{cases} \qquad (4.32b)$$

$\alpha^* < \alpha < \pi/2$:

$$g(\theta_0) = \begin{cases} 0, & 0 \leqslant \theta_0 < \alpha \\[2mm] h_1(\theta_0;\alpha) + \dfrac{3}{16\pi^2 Q_4}\left(4\pi g_0 - 4g_4 + g_7 - \dfrac{1}{2}g_8 \cos\alpha\right), \\[2mm] \qquad \alpha \leqslant \theta_0 \leqslant \theta_0' \\[2mm] h_1(\theta_0;\alpha) + \dfrac{3}{16\pi^2 Q_4}\left(4\pi g_0 - 4g_4 + g_9 - \dfrac{1}{2}g_{10} \cos\alpha\right), \\[2mm] \qquad \theta_0' \leqslant \theta_0 \leqslant 2\pi - 3\alpha \\[2mm] h_1(\theta_0;\alpha) + \dfrac{3}{16\pi^2 Q_4}\left(4\pi g_1 - 4g_5 + g_9 - \dfrac{1}{2}g_{10} \cos\alpha\right), \\[2mm] \qquad 2\pi - 3\alpha \leqslant \theta_0 \leqslant \theta_0'' \\[2mm] h_1(\theta_0;\alpha) + \dfrac{3}{16\pi^2 Q_4}\left(4\pi g_1 - 4g_5 + 2g_6 + g_9 - \dfrac{1}{2}g_{10} \cos\alpha\right), \\[2mm] \qquad \theta_0'' \leqslant \theta_0 \leqslant 2\alpha \end{cases} \qquad (4.32c)$$

The angle $\alpha^* = 1.28619...$ is the solution of the equation $2\pi - 3\alpha = \theta_0''(\alpha)$. Furthermore, the integrals g_n ($n = 4, 5,..., 10$) are defined as

$$g_4 = \int_\alpha^{2\alpha} f(\theta_1; \alpha) \, \beta(\theta_0, \theta_1; \alpha) \sin \theta_1 \, d\theta_1 \tag{4.33a}$$

$$g_5 = \int_\alpha^{2\pi - \theta_0 - \alpha} f(\theta_1; \alpha) \, \beta(\theta_0, \theta_1; \alpha) \sin \theta_1 \, d\theta_1 \tag{4.33b}$$

$$g_6 = \int_\alpha^{\psi''} [2f(\theta_1; \alpha) - f(\theta_0; \alpha)][-\tau_0 + \tau_1 - \mu(\theta_0, \theta_1; \alpha)] \sin \theta_1 \, d\theta_1 \tag{4.33c}$$

$$g_7 = \int_\alpha^{2\alpha} \left[2f(\theta_1; \alpha) - f(\theta_0; \alpha) + \frac{\pi}{2} \right]$$
$$\times [\tau_0 + \tau_1 - \delta(\theta_0, \theta_1; \alpha)] \sin \theta_1 \, d\theta_1 \tag{4.33d}$$

$$g_8 = \int_\alpha^{2\alpha} \sin \theta_1 \, d\theta_1 \int_\delta^{\tau_0 + \tau_1} (2\phi_1 + \xi_{10}) \, d\phi_1 \tag{4.33e}$$

$$g_9 = \int_\alpha^{\psi'} \left[2f(\theta_1; \alpha) - f(\theta_0; \alpha) + \frac{\pi}{2} \right]$$
$$\times [\tau_0 + \tau_1 - \gamma(\theta_0, \theta_1; \alpha)] \sin \theta_1 \, d\theta_1 \tag{4.33f}$$

$$g_{10} = \int_\alpha^{\psi'} \sin \theta_1 \, d\theta_1 \int_\gamma^{\tau_0 + \tau_1} (2\phi_1 + \xi_{10}) \, d\phi_1 \tag{4.33g}$$

For $\alpha > \pi/2$ we find

$$g(\theta_0) = \begin{cases} 0, & 0 \leqslant \theta_0 < \alpha \\ \dfrac{3}{32\pi^2 Q_4} (g_{11} - g_{12} \cos \alpha), & \alpha \leqslant \theta_0 \leqslant \theta_0'' \\ 0, & \theta_0'' \leqslant \theta_0 \leqslant \pi \end{cases} \tag{4.34}$$

where

$$g_{11} = \int_\alpha^{\bar\psi} [-\pi + 6\pi \cos \alpha + 2f(\theta_0; \alpha) + 4f(\theta_1; \alpha)]$$
$$\times (2\pi - \tau_0 - \tau_1 - \mu) \sin \theta_1 \, d\theta_1 \tag{4.35a}$$

$$g_{12} = \int_\alpha^{\bar\psi} \sin \theta_1 \, d\theta_1 \int_\mu^{2\pi - \tau_0 - \tau_1} (2\phi_1 + \xi_{10}) \, d\phi_1 \tag{4.35b}$$

Beyond the self-confinement threshold, the long-range vanishing of the RDF is observed as in the three-particle case.

As far as the triplet distribution function (TDF) is concerned, we note that its evaluation for the $N = 4$ case is tantamount to the calculation of Ω_4:

$$g_3(\theta_0, \theta_1, \phi_1) \equiv \left(1 - \frac{1}{4}\right)\left(1 - \frac{2}{4}\right) \frac{\int d\Omega_4 \, e^{-\beta V(1,2,3,4)}}{4\pi Q_4}$$

$$= \frac{3}{32\pi Q_4} \, \Omega_4(\theta_0, \theta_1, \phi_1; \alpha) \tag{4.36}$$

5. DISCUSSION

The configurational integral was computed numerically with a pace of half a degree over the whole range of α. The integrals involved in the expression of Q_4 were evaluated with a precision of four significant figures. In Fig. 7 we plot Q_N for $N = 2$, 3, and 4 calottes as a function of the packing fraction $\eta = \frac{1}{2}N[1 - \cos(\alpha/2)]$. The dots refer to an *independent* estimate of Q_4 which was obtained by means of a Monte Carlo technique. The numerical experiment was performed by dropping four calottes on the sphere at random and then computing the configurational integral as the α-dependent probability of generating a configuration with no overlap. We
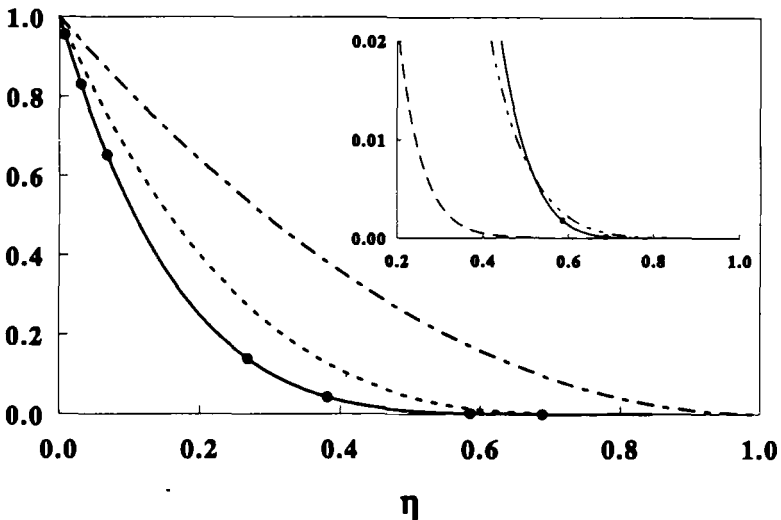
Fig. 7. Configurational integral for two (- · -), three (- -), and four calottes (—) plotted as a function of the packing fraction η. Solid circles are the results of a Monte Carlo calculation for $N = 4$. The inset shows the comparison between Q_4 (—) and the corresponding quantity for four parallel squares on a plane with periodic (- · -) and rigid boundary conditions (- -).

found that this direct numerical estimate reproduces the analytical result to within the precision of the calculation, thus confirming the results found in the preceding section.

The inset in Fig. 7 shows how the present Q_4 compares with the configurational integral of four hard *parallel* squares (with side length σ) on a plane under rigid and periodic boundary conditions.[11] Also in this finite system it is possible to identify a self-confinement threshold which falls at a packing fraction $\eta_{sq} = 4/9$ and is topologically equivalent to the phenomenon occurring on the sphere for $\eta_{cal} = 2 - \sqrt{2}$. This event produces a cusplike singularity in the pressure equation of state of four squares with periodic boundary conditions. A functional signature is also present in the relevant statistical properties of four calottes for $\eta = \eta_{cal}$: this signature is rather weak in the configurational integral whose third derivative just inflects for $\alpha = \pi/2$, but is more apparent in the RDF profile, which, beyond the above threshold, vanishes over a finite range of distances [see Eq. (4.34)]. The functional change is sharper for the squares because of the shape and the alignment constraint, which also shift the transition to lower packing fractions.

It is interesting to compare the self-confinement threshold of the four-calotte system with the percolation density of the excluded volume.[12] This
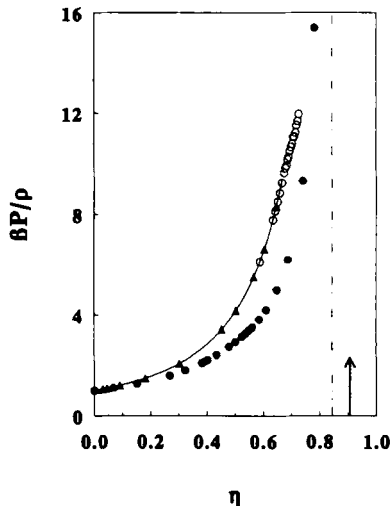
Fig. 8.   Compressibility factor $\beta P/\rho$ of calottes on a sphere plotted as a function of the packing fraction η: solid circles, four calottes; open circles, 2000 calottes.[8] The corresponding quantity for disks on a plane[12] is also shown for comparison (solid triangles). The continuous line is based on the truncated six-term virial expansion for disks.[12] The vertical line represents the close-packing threshold of four calottes, while the arrow indicates the corresponding limit attained in the hexagonal tessellation of the plane $\eta_{CP} = \pi/(2\sqrt{3})$.

quantity signals the occurrence of the first spanning cluster of overlapping exclusion spheres. For hard disks this transition takes place at a packing fraction $\eta_P^{(HD)} \simeq 0.22$.[13] Even if the percolation threshold is properly defined only for an infinite system, we can still evaluate this quantity for a finite system by calculating the density above which it is no longer possible to find a configuration that shows disconnected pieces of excluded volume. In the present model, the largest diameter of the hosting sphere which is consistent with a disconnected excluded volume can be plausibly associated with a configuration where three calottes touch one another, while the fourth stays as far as possible from the close-packed triangular cluster. Another possibility might be that where the four particles form two distinct pairs of kissing calottes tilted at a 90° angle. A simple calculation yields for α a value of 69°.44 for the former configuration and 67°.02 for the latter. The largest value is tantamount to a packing fraction $\eta_P^{(4)} = 0.356$. This threshold also corresponds to the density beyond which the accessible volume on the spherical surface breaks into separate cavities.[12,13] The volume of such cavities shrinks to zero as soon as α grows beyond 90° (which is, in fact, the largest angular diameter available to five equal non-overlapping calottes).

The compressibility factor of four calottes is compared in Fig. 8 with the corresponding quantity for 2000 calottes[8] and for a fluid of hard disks.[14] As expected, the lower average coordination number in the smaller system generally results in a lower pressure: however, at very high densities the two curves will eventually cross each other because the surface fraction covered by four close-packed calottes is lower than in the infinite system.

In Fig. 9 we present the radial distribution function for increasing densities. As in the three-particle case, we checked that the RDF is properly
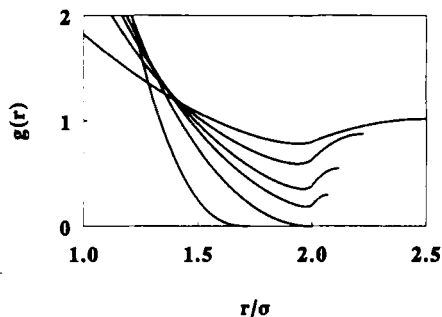
Fig. 9.   Radial distribution function of four calottes plotted as a function of r/σ for increasing values of α. From top to bottom (with reference to the tail of the RDF), $\alpha = 72°$, 81°, 85°, 87°, 90°, 95°.
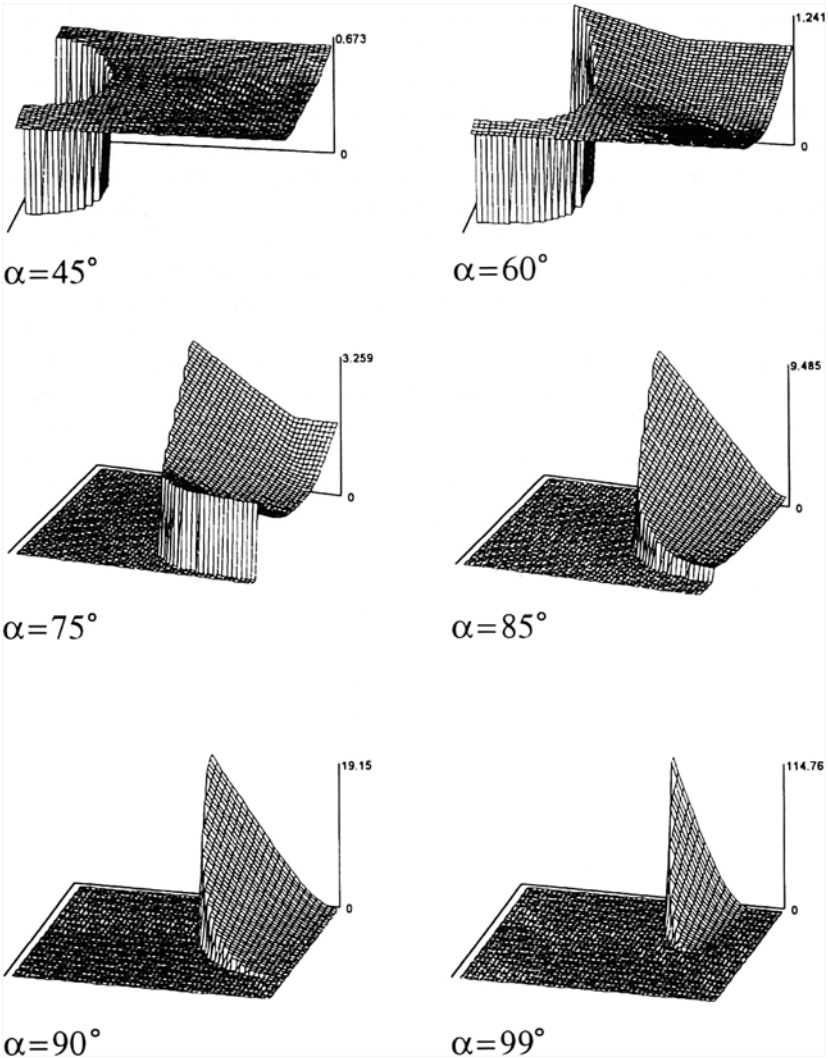
Fig. 10. Triplet distribution function of four calottes plotted as a function of the polar angles of particle 3 (θ_1, ϕ_1), while particles 1 and 2 are kept fixed at angular distance $\theta_0 = \arccos(-1/3)$. The θ_1 axis points toward the reader and ranges between α and π (from top to bottom) since the function vanishes for $\theta_1 < \alpha$. The ϕ_1 axis is the horizontal one and ranges between 0 and π (from left to right). The number on top of the vertical axis gives the maximum value of the function. The complete representation of $g_3(\theta_0, \theta_1, \phi_1)$ would involve a mirror image of each graph corresponding to values of ϕ_1 ranging between π and 2π.

normalized. We note that the first spatial derivative shows a cusp singularity for $r/\sigma = 2$.

Figure 10 shows a series of surface plots representing the four-calotte TDF $g_3(\theta_0, \theta_1, \phi_1)$ for $\theta_0 = \arccos(-1/3)$. We note that for $\alpha > \pi/2$ the domain where $g_3(\theta_0, \theta_1, \phi_1) \neq 0$ splits into two disjoint regions as a result of particle confinement (see Section 4.2). It is customary to contrast the TDF with the *reference* Kirkwood superposition approximation (KSA).[15] We verified that KSA overestimates triplet correlations all over the density range. The resulting TDF, while being systematically more peaked and sharper, still qualitatively reproduces the overall shape of the exact function with one rather notable exception: it fails to signal the ergodicity threshold for $\alpha = \pi/2$. In fact, according to KSA, at the above density and even beyond particles might still "tunnel" between the two regions of the spherical surface which correspond to the sharp twin peaks that are observed in the TDF. Such a failure of KSA quite clearly arises from the incorrect sampling of the intersection region common to three extended calottes which is not reducible to the mere propagation of two-body effects.

6. CONCLUDING REMARKS

In this paper we have investigated the thermodynamics of a "toy" model which allows an exact analysis of the interplay between statistics and excluded-volume geometry. The most relevant feature which is somehow elucidated even in such a crude caricature of a real system is the onset of a topological transition corresponding to the self-confinement of particles on the sphere. We surmise that the corresponding "locking" of the structure is the underlying precursory mechanism that makes the *freezing* of the fluid the necessary outlet for a densely packed hard-core system in the thermodynamic limit. We plan to discuss in a forthcoming paper some aspects of the model related to entropy and multiparticle correlations in the light of some recent suggestions pertaining to the freezing of fluids in three dimensions.[16,17]

REFERENCES

1. P. M. L. Tammes, *Recl. Trav. Bot. Néerl.* **27**:1 (1930).
2. L. Fejes Tóth, *Jahresber. Deutsch. Matematikerverein.* **53**:66 (1943); H. S. M. Coxeter, *Trans. N.Y. Acad. Sci. Ser. II* **24**:320 (1962); A. L. Mackay, J. L. Finney, and K. Gotoh, *Acta Cryst. A* **33**:98 (1977); D. A. Kottwitz, *Acta Cryst. A* **47**:158 (1991), and references therein.
3. K. W. Kratky, *J. Comput. Phys.* **21**:205 (1980); see also W. Schreiner and K. W. Kratky, *J. Chem. Soc. Faraday Trans. 2* **78**:379 (1982).
4. K. W. Kratky, *J. Stat. Phys.* **25**:619 (1981).
5. A. J. Post and E. D. Glandt, *J. Chem. Phys.* **85**:7349 (1986).
6. A. J. Post and E. D. Glandt, *J. Chem. Phys.* **88**:5805 (1988).
7. J. Tobochnik and P. M. Chapin, *J. Chem. Phys.* **88**:5824 (1988).
8. S. Prestipino Giarritta, M. Ferrario, and P. V. Giaquinta, *Physica A* **187**:456 (1992); **201**:649 (1993).
9. L. A. Rosen, N. A. Seaton, and E. D. Glandt, *J. Chem. Phys.* **85**:7359 (1986).
10. S. Prestipino Giarritta, Tesi di Dottorato, University of Messina (1993).
11. W. G. Hoover and B. J. Alder, *J. Chem. Phys.* **46**:686 (1967).
12. K. W. Kratky, *J. Stat. Phys.* **52**:1413 (1988).
13. W. G. Hoover, N. E. Hoover, and K. Hanson, *J. Chem. Phys.* **70**:1837 (1979).
14. J. J. Erpenbeck and M. Luban, *Phys. Rev. A* **32**:2920 (1985).
15. J. G. Kirkwood, *J. Chem. Phys.* **3**:300 (1935).
16. P. V. Giaquinta, G. Giunta, and S. Prestipino Giarritta, *Phys. Rev. A* **45**:6966 (1992).
17. P. V. Giaquinta and G. Giunta, *Physica A* **187**:145 (1992).